

Instability of plastic deformation as a self-organizing fractal

A. M. Avdeenko and E. I. Kuzko

Moscow State Steel and Alloys Institute, Moscow, Russia

(Received 4 March 1999; revised manuscript received 23 June 2000; published 19 January 2001)

The collective dynamics of plastic deformation is investigated using a field approach. A correlation function of displacement field fluctuations in a Cosserat-like continuum model is calculated via the renormalization group method. The dynamics of the correlation length and mean-squared deviation of displacement field fluctuations are parameterized by a dimensionless strain-hardening rate. The value of the critical index was obtained experimentally from the surface profiles of steel and copper specimens measured during plastic tension. The results allow one to predict the point of plastic flow instability at given conditions.

DOI: 10.1103/PhysRevB.63.064103

PACS number(s): 62.20.Fe, 83.50.-v, 46.05.+b, 46.15.Ff

I. INTRODUCTION

The structure of real polycrystalline material during the plastic deformation process evolves on different length scales sequentially (from the microscopic up to the macroscopic scale) and simultaneously. There exist “basic defects”—plastic flow carriers—of various sizes: dislocations are microstructural elements, dislocation superstructures (including disclinations) represent a mesoscopic length scale, and plastic and rotational modes are of a macroscopic scale.

Concentration and coupling of defects increase during plastic deformation of the initial structure.¹ The emergence of new degrees of freedom (carriers of the next, “higher” level) is a result of the self-organization of previous level carriers.² The process of plastic deformation is accompanied by microfracturing and followed by macroscopic failure. Fracture processes, on the other hand, can be treated as the appearance and development of some “basic objects,” forming the whole hierarchy of defects: microcracks, voids, facets of the grain boundary fracture, and so on. Microcracks join up under stress to form mesoscopic defects and, finally, a single macroscopic crack suppressing the development of others.

Some theoretical arguments and experimental facts enable us to describe self-organization in plastically deformed and fractured structures in a unified way. We propose a general approach based on three main principles: (i) “universality,” the given set of external parameters (stress, strain limit, etc.) always causes the loss of flow macrostability, followed by mechanical failure; (ii) “divergence of characteristic scales,” the characteristic lengths of “basic elements” of plastic flow and fracture exceed all essential microscopic length scales for the critical values of stress or strain; (iii) “scaling” (fractality), the properties of strain field statistics and crack surface topology obey scaling laws.

The main goal of the present investigation is to describe some plastic deformation phenomena as a result of the evolution of an extended dissipative dynamical system and to study the relations between the statistics of the media and the parameters of the plastic flow self-organization. The same methodology applied to the case of fracture will be presented in the near future.

II. MODEL AND SOLUTION

We consider a solid under stress as the three-dimensional volume Ω_d ; the system of external forces applies to its boundary. The area Ω_d is subdivided into N small cubic cells v_i ; for each of them a field of displacement A_μ ($\mu=1,2,3$) is defined as a displacement of site v_i from initial r_i to the stressed-state r'_i position: $A_\mu = r'_i - r_i$. Since the initial state and local properties are unknown and N is huge ($v_i \ll \Omega_d$), we will use a statistical approach to solve the problem. The $3N$ -dimensional distribution $f(A_\mu(i))$ for $N \rightarrow \infty$ is presentable as

$$f[A_\mu] = e^{W[A_\mu]}, \quad (1)$$

where $W[A_\mu]$ can be called the generating functional of an open system.

We will limit our consideration to such a class of media for which the state in the vicinity of point r_i at time t_i is determined by spatial derivatives of the displacement field A_μ specified for any time τ_i being $t_0 < \tau_i < t_i$, where t_0 is the start of evolution. Barely taking inertial terms into account, Eq. (1) may contain the temporal derivative (not greater than that of the first order) of a displacement field.

For a macroscopically isotropic and homogeneous solid (by initial conditions, i.e., no external stress), the generating functional can be expressed, in general, as a functional polynomial

$$W[A_\mu] = \int \cdots \int \sum_{k=2}^{\infty} \frac{V_k^{\mu \cdots \nu}(r_i, t_i)}{k} A_{\mu,p} \cdots A_{q,\nu} \\ \times dr_1 dt_1 \cdots dr_i dt_i \cdots,$$

where $V_k^{\mu \cdots \nu}(r_i, t_i)$ ($i=1, \dots, k, \dots$) are real tensors of rank $2k$.

Let first k indices ($\mu=1,2,3$) denote A_μ components, the next k indices ($\mu=0,1,2,3$) derivatives. The distribution $f[A_\mu]$ is a monotone function of $W[A_\mu]$: hence the most probable process corresponds to a path \bar{A}_μ or $\bar{A}_{\mu,\nu}$ ($\mu=1,2,3$) satisfying the variational equation

$$\frac{\delta W[A_\mu]}{\delta A_\mu} = 0$$

and given initial and boundary conditions.

The solution $\bar{A}_\mu(\bar{A}_{\mu,\nu})$ and difference $\delta A_{\mu,\nu} = A_{\mu,\nu} - \bar{A}_{\mu,\nu}$ can be regarded as a ‘‘classic’’ path and fluctuations, respectively. We restrict our attention to the so-called ‘‘active’’ paths assuming $ds/dt \geq 0$ for each point (\mathbf{r}, \mathbf{t}) , where

$$s = \int_{t_0}^t \left(\frac{\partial \bar{A}_{\mu,\nu}}{\partial t} \frac{\partial \bar{A}^{\mu,\nu}}{\partial t} \right)^{1/2} d\tau$$

is some internal parameter of a system, the ‘‘length’’ of the classic path, and evolution along this ‘‘classic’’ path is the same for all cells v_i .

To build a generating functional of fluctuations of field $A_{\mu,\nu}$ we produce a series expansion of $W[A_\mu]$ in the vicinity of $\bar{A}_{\mu,\nu}$. As is well known, it is possible to express the derivatives with respect to the time of an arbitrary order in terms of functions of internal parameters: length of a path s , scalar curvatures $\vartheta_1(s) \cdots \vartheta_{n-1}(s)$, and torsion $\vartheta_n(s)$ (n is the number of independent components of tensor $\bar{A}_{\mu,\nu}$).

For paths $ds/dt \geq 0$ integration over the spatial variables gives unessential constants, proportional to some powers $(\Omega_d)^n$; temporal integration parametrizes vertices $V_k^{\mu \cdots \nu}$ by $s, \vartheta_1(s) \cdots \vartheta_{n-1}(s), \vartheta_n(s)$. In the case of proportional stress $\vartheta_n(s) \equiv 0$ tensor $V_k^{\mu \cdots \nu}$ depends only on the second invariant of $\bar{A}_{\mu,\nu}$: $V_k^{\mu \cdots \nu} = V_k^{\mu \cdots \nu}(s)$.

Let $W[A_\mu]$ be the generating functional of fluctuations with vertices $V_k^{\mu \cdots \nu}(r_i, t_i, s, \vartheta_n(s))$. Normalized averages weighted by $e^{W[A_\mu]}$ are the correlation functions of order $2k$:

$$\begin{aligned} R_{2k}^{\mu \cdots \nu}(r_i, t_i) &= \langle A^{\mu,q}(r_1, t_1) \cdots A^{p,\nu}(r_{2k}, t_{2k}) \rangle \\ &= \frac{1}{Z} \int A^{\mu,q}(r_1, t_1) \cdots A^{p,\nu}(r_{2k}, t_{2k}) e^{W[A_\mu]} dA_\mu, \\ Z &= \int e^{W[A_\mu]} dA_\mu, \end{aligned} \quad (2)$$

where dA_μ stands for continuum integration.

This relation shows that, in principle, the statistics of the deformation field fluctuations can be parametrized with the set of curvature and torsion characteristics for a ‘‘classic’’ path. We denote Fourier representations as $A_\mu(p, \omega)$, $V(p, \omega)$. The modes $\omega \neq 0$ we call ‘‘fast’’; the ‘‘slow’’ generating functional is

$$W'[A_\mu] = -\ln \frac{1}{Z} \int e^{W[A_\mu]} d'A_\mu,$$

where $d'A_\mu$ is the sign of the ‘‘fast variable’’ continuum integration. Further we omit the prime.

We define the inverse to the free correlation function $R_{20}^{\mu \cdots \nu}(r)$ operator $\int V_2^{ppqq}(r_1, r_1') R_{20,mpqn}(r_1' - r_2) dr_1' = \delta_m^\mu \delta_n^\nu \delta(r_1 - r_2)$ and call it the free vertex of second order.

For systems where $V_k^{\mu \cdots \nu}(r_i) = 0$ ($k > 2$) the free vertex of second order coincides with vertex $V_2^{\mu \cdots \nu}(r_i)$.

In a general case, when $V_k^{\mu \cdots \nu}(r_i) \neq 0$ ($k > 2$), then the normalized bilocal average weighted by e^{-W} determines the full correlation function $R_2^{\mu \cdots \nu}(r)$. The operator $V_2^{\mu \cdots \nu}(r_i)$,

inverse to the full correlation function, is definable by Eq. (2) with the substitution $R_{20}^{\mu \cdots \nu}(r) \rightarrow R_2^{\mu \cdots \nu}(r)$. This quantity includes interactions (nonlinear phenomena) and will be called the full vertex of second order. The full vertex, in general, does not coincide with the operator for the squares of field variables in generating functional (1), denoted by $V_{20}^{\mu \cdots \nu}(r_i)$.

We assume that for the initial state (there is no external stress) the ‘‘classic’’ path corresponds to the equilibrium equation of the Cosserat elastic pseudocontinuum model:³⁻⁶

$$\nabla^2 A_\mu + \frac{1}{1-2\nu} \nabla_\mu (\nabla_\nu A^\nu) - \xi_0^2 \nabla^2 (\nabla^2 A_\mu - \nabla_\mu \nabla^\nu A_\nu) = 0,$$

where ξ_0 is the structural length scale of the elastic pseudocontinuum,

$$\nabla_\mu = \frac{\partial}{\partial x_\mu}, \quad \nabla^2 = \sum_{\mu=1}^3 \frac{\partial^2}{\partial x_\mu^2}.$$

The field A_μ contains longitudinal and transverse components, $A_\mu = A_\mu^n + A_\mu^t$, and corresponding distortions, $A_{\mu,\nu}^n = (1/n) \delta_{\mu,\nu} A_{k,k}$ (n is the number of components of field A_μ) and $A_{\mu,\nu}^t = A_{\mu,\nu} - A_{\mu,\nu}^n$. The longitudinal and transverse terms of the free vertex of second order, $V_{20}^{\mu \cdots \nu}(r_i) = V_{20}^{\mu \cdots \nu,n}(r_i) + V_{20}^{\mu \cdots \nu,t}(r_i)$, are

$$V_{20}^{\mu \cdots \nu,n}(r_i, s \rightarrow +0) = \frac{T_2^{\mu \cdots \nu,n}}{V \langle \varepsilon_2^2 \rangle} \delta(r_1 - r_2),$$

$$V_{20}^{\mu \cdots \nu,t}(r_i, s \rightarrow +0) = \frac{T_2^{\mu \cdots \nu,t}}{V \langle \varepsilon_1^2 \rangle} [1 + \xi_0^2 \nabla^2] \delta(r_1 - r_2),$$

where

$$\langle \varepsilon_1^2 \rangle = V^{-1} \int R_{20\mu\nu}^{\mu\nu,t}(r) dr,$$

$$\langle \varepsilon_2^2 \rangle = V^{-1} \int R_{20\mu\nu}^{\nu,n}(r) dr$$

are longitudinal and transverse mean-square deviations of strain fields fluctuations at state $s \rightarrow +0$, V is the volume, $T_2^{\mu \cdots \nu,n} = (e^n)^2 (e^\nu)^2$, $T_2^{\mu \cdots \nu,t} = \delta^{\mu q} e^p e^\nu$, and e^q is the unit vectors in direction r .

It is possible to show that the stressed-state free vertices of longitudinal fluctuations are the same, whereas the free vertices of transverse fluctuations have the form

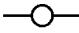


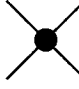
$$V_{20}^{\mu \cdots \nu,t}(r_i, s) = \frac{T_2^{\mu \cdots \nu,t}}{V \langle \varepsilon_1^2 \rangle} [\theta(s) + \xi_0^2 \nabla^2] \delta(r_1 - r_2),$$

where $\theta(s) = G^{-1} d\tau/ds$ is the shear strain-hardening rate along the ‘‘classic’’ path normalized by the shear modulus and controlled by the internal geometry of the ‘‘classic’’ path—by its length s , curvature, and torsion.

The corresponding correlation functions are given by

$$R_{20}^{\mu \cdots \nu,t}(r, s) = \frac{C_2^{\mu \cdots \nu,t} V \langle \varepsilon_1^2 \rangle}{4 \pi r \xi_0^2} e^{-r/\xi},$$

TABLE I. The basic elements of the Feynman diagram.

$V_{20}^{\mu\dots\nu}(p)$	$V_2^{\mu\dots\nu}(p)$	$V_4^{\mu\dots\nu}$	$\bar{g}_4^{\mu\dots\nu}(p_i)$
			

$$R_{20}^{\mu\dots\nu,n}(r,s) = C_2^{\mu\dots\nu,n} V \langle \varepsilon_2^2 \rangle \delta(r_1 - r_2),$$

where $C_2^{\mu\dots\nu,t} = \delta^{\mu q} e^p e^v$, $C_2^{\mu\dots\nu,n} = e^\mu e^\mu e^v e^v$, and $\xi = \xi_0 \theta^{-1/2}$ is the correlation length of transverse displacement fluctuations.

Mean-square deviations of transverse and longitudinal displacement fields fluctuations can be expressed as, respectively,

$$\langle \varepsilon^2(\theta) \rangle = V^{-1} \int R_{20\mu\nu}^{\mu\nu,t}(r,\theta) dr = \langle \varepsilon_1^2 \rangle \theta^{-1},$$

$$\langle \varepsilon^2(\theta) \rangle = V^{-1} \int R_{20\mu\nu}^{\mu\nu,n}(r,\theta) dr = \langle \varepsilon_2^2 \rangle,$$

and, except the narrow macroelasticity region where $\theta \ll 1$ and $\langle \varepsilon_1^2 \rangle \approx \langle \varepsilon_2^2 \rangle$, then $\langle \varepsilon^2(\theta) \rangle \gg \langle \varepsilon_2^2 \rangle$. We will limit our consideration of the statistics of displacement field fluctuations to transverse terms; the sign “ t ” will be omitted in the following.

We call $\langle \varepsilon_1^2 \rangle$ and ξ_0 the normalized mean-square deviation of displacement field fluctuations and fundamental length scale, respectively. The formal definition is

$$\langle \varepsilon_1^2 \rangle = \lim_{\theta \rightarrow 1-0} \langle \varepsilon^2(\theta) \rangle,$$

$$\xi_0 = \lim_{\theta \rightarrow 1-0} \xi(\theta);$$

experimental investigations of displacement fluctuation statistics (extrapolated to the area $s \rightarrow +0$) can be used to estimate numerical values. The approximation $\xi_0 \rightarrow 0$ is the case of the usual continuum considerations of elasticity and plasticity.

The media $V_k^{\mu\dots\nu} \neq 0$, ($k > 2$) we will call the nonlinear Cosserat pseudocontinuum; the generating functional $W[A_\mu]$ corresponds to the statistics of displacement field fluctuations.

In general, the calculation of the full correlation functions $R_{2k}^{\mu\dots\nu}(p)$ [normalized averages weighted by $e^{-W[A_\mu]}$ for $V_k^{\mu\dots\nu} \neq 0$ ($k=3,4,\dots$)] can be performed employing the Feynman-diagram technique. We will use the diagrams in the frequency representation: the main elements are “free” and “full” correlation functions and vertices of the order $2k$. The term “free” stands here for the vertices corresponding to a given set of wave vectors on external lines and to the parameterized “classic” path $\theta(s, \vartheta_n(s))$. The basic elements of the Feynman diagram used are shown in Table I.

System (2) resolved with respect to vertices thus looks like

$$\text{Full vertex} = \text{Free vertex} + \text{Loop diagram} + \dots$$

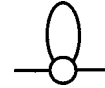
$$\text{Four-point full vertex} = \text{Four-point free vertex} + \text{Four-point loop diagram} + \dots$$

(3)

Introducing $d^2(p) = R_2(p)/R_{20}(p)$ we then use effective vertices defined as

$$\bar{g}_k(p_i) = V_k(p_i) \prod_{i=1}^k d(p_i).$$

Calculation of



at first order in interactions performed in the scale-regularization formalism.⁷ The solution of relevant renormalization group (RG) equation for θ gives the expression for the mean-square deviation and correlation length in the form of

$$\langle \varepsilon^2(\theta) \rangle = \langle \varepsilon_1^2 \rangle \theta^{-\alpha},$$

$$\xi(\theta) = \xi_0 \theta^{-\alpha/2}, \quad (4)$$

where $\alpha = 1 - a_1 g_4$, $a_1 = (n+2)/4$, and n is the number of independent components of field $A_{\mu,\nu}$. The active deformation process is accompanied by a decrease in the strain-hardening rate ($d\theta/ds \leq 0$); hence the mean-square deviation of displacement fluctuations and correlation length increase according to the scaling law (4) satisfying the rule

$$\frac{\langle \varepsilon^2(\theta) \rangle}{\xi^2(\theta)} = \frac{\langle \varepsilon_1^2 \rangle}{\xi_0^2}. \quad (5)$$

Thus, if $\langle \varepsilon^2(\theta_1) \rangle$, $\xi(\theta_1)$ are mean-square deviations of fluctuations and correlation length for state θ_1 , then

$$\langle \varepsilon^2(\theta) \rangle = \langle \varepsilon^2(\theta_1) \rangle \left(\frac{\theta}{\theta_1} \right)^{-\alpha},$$

$$\xi(\theta) = \xi(\theta_1) \left(\frac{\theta}{\theta_1} \right)^{-\alpha/2}.$$

In other words, the introduction of a new fundamental scale $\xi(\theta_1)$ and the mean-square deviation $\langle \varepsilon^2(\theta_1) \rangle$ is equal to the scale transformation $\theta \rightarrow (\theta/\theta_1)$. Regardless of the choice of a normalizing point, the limit $\theta \rightarrow 0$ leads to $\langle \varepsilon^2(\theta) \rangle, \xi(\theta) \rightarrow \infty$ —cooperative effects arise. As $\langle \varepsilon^2(\theta) \rangle, \xi(\theta)$ increase, for some $\theta \leq \theta_1$ fluctuations become comparable to the mean deformation ($\langle \varepsilon^2 \rangle \approx s^2$) or the correlation length reaches the size of a system ($2\xi \approx L_0$)—homogenous deformation considered in conventional plasticity theories⁸ becomes unstable. For example, uniaxial strain leads to the formation of a transverse neck (where the specimen fails afterwards), so an estimation of the flow instability is roughly

$$\theta_* = \left(\frac{L_0}{2\xi_0} \right)^{-2/\alpha}, \quad (6)$$

where L_0 is the smallest specimen dimension (thickness).

For $\theta \geq \theta_*$ plastic waves propagate along a specimen: for $\theta < \theta_*$ spatial fluctuations of the displacement field interfere, forming macroscopic localizations of the flow.

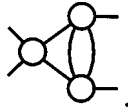
Equation (3) for \bar{g}_4 at second order in the interaction is

$$\theta \frac{d\bar{g}_4}{d\theta} = b_1 \bar{g}_4^2,$$

where $b_1 = (n+8)/4$. This, along with the equation for $V_2(\theta)$, gives an effective contribution of the second order to the correlation length and mean-square deviation of the displacement field fluctuations:

$$\begin{aligned} \langle \varepsilon^2(\theta) \rangle &= \langle \varepsilon^2(\theta_1) \rangle \theta^{-\alpha(\theta)}, \\ \xi(\theta) &= \xi(\theta_1) \theta^{-\alpha(\theta)/2}, \\ \alpha(\theta) &= 1 + \frac{1}{b_1} \frac{\bar{g}_4(\theta)}{g_4}, \\ \bar{g}_4(\theta) &= g_4 (1 - b_1 g_4 \ln \theta)^{-1}. \end{aligned} \quad (7)$$

For $g_4 < 0$ the deformation process (strain-hardening rate decreases) is accompanied by an infinitely increasing interaction. In the vicinity $|g_4 \ln \theta| \approx 1/b_1$, the next (third) order of perturbation theory should be considered. Only one correction is sufficient here, namely,



The associated RG equation is

$$\theta \frac{d\bar{g}_4}{d\theta} = b_1 \bar{g}_4^2 - b_2 \bar{g}_4^3,$$

where $b_2 = (n+8)(n+1)/2$. The solution, in its implicit form, may be used for numerical approximations. The fixed point for this equation is $g_4^c = -b_1/b_2$; if $n=3$, then $g_4^c = -0.125$, so for $g_4 < 0$ the scaling law is asymptotically universal:

$$\langle \varepsilon^2(\theta) \rangle = \langle \varepsilon_1^2 \rangle \theta^{-\alpha_*}, \quad \xi = \xi_0 \theta^{-\alpha_*/2}, \quad \alpha_* = 1 - a_1 g_4^c > 1.$$

According to Eq. (7) for the case of negative interactions ($g_4 > 0$) the decrease of the strain-hardening rate on the deformation path is accompanied by a decrease of the interaction intensity and $\theta \rightarrow 0, \bar{g}_4 \rightarrow 0$. The critical index $\alpha \rightarrow 1$ and the law for the correlation length and mean-square deviation divergence is universal again:

$$\langle \varepsilon^2(\theta) \rangle = \langle \varepsilon_1^2 \rangle \theta^{-1}, \quad \xi = \xi_0 \theta^{-1/2};$$

different types of universality correspond to different signs of the g_4 value.

Expanding the k th-order vertex in the vicinity of the ‘‘classic’’ path to the functional Fourier series, it is possible to prove a relation between the interaction in reduced variables, renormalized to the state $s \rightarrow +0$, and the stress-strain diagram⁹

$$g_{m+2} = d_{m+2} \langle \varepsilon_1^2 \rangle \mu^{m+2} (\Omega_d)^{m/2},$$

where $d_m = d^m \theta / ds^m$ is a ‘‘parabolicity’’ of the stress-strain curve. For only one nonvanishing vertex, $g_4 = \langle \varepsilon_1^2 \rangle d_4$; i.e., the sign of the interaction is determined by the sign of d_4 .

Ultraviolet analysis [$p^2 \geq \mu^2 \theta(s, \vartheta_n(s))$] is performed using the same method. The diagram corresponding to the first significant ultraviolet correction is



Solving the RG equation in the ultraviolet area gives the full correlation function in the form

$$\begin{aligned} R_2(p) &= \langle \varepsilon^2(\theta) \rangle \left(\frac{p^2}{\mu^2 \theta} \right)^{-\beta}, \\ \beta &= 1 - a_3 g_4^2, \quad a_3 = \frac{n+2}{8}. \end{aligned} \quad (8)$$

We introduce a correlation (fractal) dimension $D = 2\beta$ as a dimension of the correlation function of displacement fluctuations. Higher orders are evaluated similarly; omitting simple evaluations, we barely state here the main result: in the case $g_4 < 0$ increasing p^2/θ ratio enlarges the absolute value of the interaction g_4 and, therefore, reduces the dimension. For the case $g_4 > 0$ an increase of the ratio p^2 to θ weakens the interaction and, hence, increases the dimension: for $p^2 \rightarrow \infty, g_4 \rightarrow 0$ and $D \rightarrow 2$.

To summarize, the statistics of displacement field fluctuations may be expressed in terms of (i) the strain-hardening rate $\theta(\vartheta_n(s), s)$, which is governed by active deformation along the ‘‘classic’’ path; (ii) intrinsic constants of the media: structure length scale ξ_0 (associated with the elastic unload of constrained deformation) and parameter g_4 representing the magnitude of interaction between the fluctuations of the flow, expressible through a ‘‘parabolicity’’ of the stress-strain diagram and reduced mean-square deviation (7). In the asymptotic area $\theta \rightarrow 0$ the statistics of fluctuations exhibits fractal behavior: the correlation length and displacement heterogeneity diverge according to a power law, being connected to each other by the similarity relationship.

The results obtained constrain the ability of the analytic plasticity theory: the assumption of a possibility for the me-

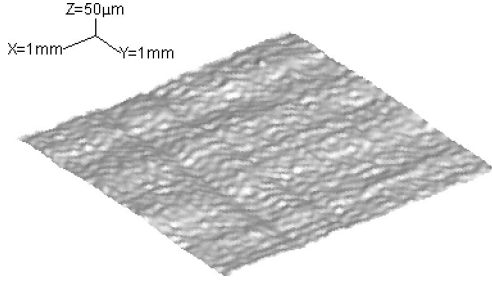


FIG. 1. Lateral side of a steel specimen. Elevation profile at strain $\varepsilon = 0.32$.

dia, during active deformation, to evolve along any path (where the quasiequilibrium state of the system can be modeled) is not realistic enough. There are limitations on the “elementary” volume ξ_0^d in a field approach and on the “diagram”: in the vicinity $\theta \approx \theta_*$ the magnitude of fluctuations becomes comparable to the length of the “classic” path. In this area the concept of a deterministic description, based on some kind of equilibrium equations, makes no conventional sense, but exactly here processes governing the strength properties, namely, the loss of plastic flow stability and fracture, take place.

III. EXPERIMENTAL PROCEDURE AND RESULTS

In order to examine the correctness of the accepted assumptions and obtained results [Eqs. (4), (7), and (8)], we have performed measurements of the plastic deformation heterogeneity. In the present investigation, the heterogeneity of the displacement fields was observed during the evolution of a polished surface of steel (0.1% carbon) and copper samples, subjected to uniaxial tension at a constant strain rate $\dot{\varepsilon} = 10^{-3} \text{ s}^{-1}$ and a normal temperature 293 K, using a scanning laser profilometer technique.¹⁰

Local elevations of the lateral surface were measured at points arranged on a square lattice covering $9.6 \times 9.6 \text{ mm}^2$ area: for steel, $65 \times 65 = 4225$ points with one cell size $150 \mu\text{m} \times 150 \mu\text{m}$ (Fig. 1); for copper, $129 \times 129 = 16641$ points with $75 \mu\text{m} \times 75 \mu\text{m}$ cells. The accuracy of the method is $\pm 1.25 \mu\text{m}$ for all spatial directions. The measurement procedure was carried out at an initial state (zero strain) and for strains $s = 0.02 - 0.36$ (the range depends on the material), up to the failure of the sample. The measured elevation span changes during the deformation from $50 \mu\text{m}$ to $115 \mu\text{m}$. Vertical span achieves the minimum at some strained state ($s \leq 0.06$), *not* at an initial point. The reason is that the polished surface is “microsmooth,” *not* “macroflat;” it becomes flatter, remaining almost smooth, after a small amount of plastic deformation.

The Fourier transform of the elevation values matrix for every strain s ,

$$h_3(\mathbf{p}) = \int h_3(\mathbf{r}) e^{i\mathbf{p}\cdot\mathbf{r}} d\mathbf{r},$$

$$\mathbf{p} = \frac{2\pi\mathbf{n}}{L_0}, \quad \mathbf{n} = (n_1, n_2), \quad 0 \leq n_1, n_2 \leq \frac{N-1}{2},$$

TABLE II. Scaling parameters: index, fundamental length scale, instability transition point, and estimation of the normalized mean-square deviation.

	$\alpha/2$	ξ_0 (μm)	s_*	$\langle \varepsilon_1^2 \rangle$
Fe	0.75 ± 0.12	28 ± 2	0.12 ± 0.05	$(1-2) \times 10^{-4}$
Cu	0.06 ± 0.01	90 ± 3	0.17 ± 0.05	$(2-4) \times 10^{-4}$

was calculated using a standard algorithm. Here L_0 is the size of a measured square, h_3 is the measured height (relative to the mean plane), and the spatial wavelengths are in the range of $300 \mu\text{m}$ to 9.6 mm .

The interdependence of $h_3(\mathbf{p})$ and the function of the pair fluctuation correlation is

$$\langle h_{3,i}(\mathbf{p})/h_{3,i}(-\mathbf{p}) \rangle = C_{2,33ii} R_2(\mathbf{p}),$$

$$h_{3,i}(\mathbf{p}) = \mathbf{p}_i h_3(\mathbf{p}),$$

$i = 1, 2$, and $\langle \dots \rangle$ denotes angular averaging on the plane of spatial frequencies \mathbf{p} . The correlation length is meant to be

$$\xi = 2\pi \frac{\int R_2(\mathbf{p}) d\mathbf{p}}{\int |\mathbf{p}| R_2(\mathbf{p}) d\mathbf{p}}.$$

According to Eq. (7) the linear regression of the experimentally measured data $\ln \xi - \ln \theta$ gives the values and accuracy for ξ_0 and α . The fractal dimension of the fluctuation correlation function was determined as

$$D = -\frac{1}{2} \frac{d \ln R_2(\mathbf{p})}{d \ln p^2};$$

the values and accuracy were obtained also by a linear fit on a log-log scale. The micro- to macroinstability transition point s_* was determined using Eq. (6); half of the specimen thickness was regarded as the smallest characteristic dimension. The scaling parameters—fundamental length scale ξ_0 , index α , instability transition point s_* , and estimation of the normalized mean-square deviation $\langle \varepsilon_1^2 \rangle$ —are given in Table II.

The increase of strain is accompanied by a decrease of the strain-hardening rate and an increase of the correlation length in accordance with the scaling law, as shown in Fig. 2. The macroscopic instability transition point determined by Eq. (6), $s_* = 0.12 \pm 0.05$ for iron and $s_* = 0.17 \pm 0.05$ for copper, is considerably less than that for the usual estimate in the model of geometric fault ($s_p = m$, for Fe $s_p = 0.29$, for Cu $s_p = 0.33$) and for macrohomogenous tension ($s_p = 0.36$ for Fe, $s_p = 0.37$ for Cu).

The behavior of the fractal dimension of the correlation function during the deformation process is given in Fig. 3. Experiments show statistically reliable self-similar behavior of the displacement field fluctuations. During deformation the strain-hardening rate (for given strain values) θ decreases and the fractal dimension D increases: in iron from $D = 1.27 \pm 0.01$ for $\theta = 1.49 \times 10^{-2}$ to $D = 1.52 \pm 0.01$ for $\theta = 0.69 \times 10^{-2}$ —the effective interaction thus changes from 0.85 ± 0.04 to 0.36 ± 0.03 . Determined from D , the absolute

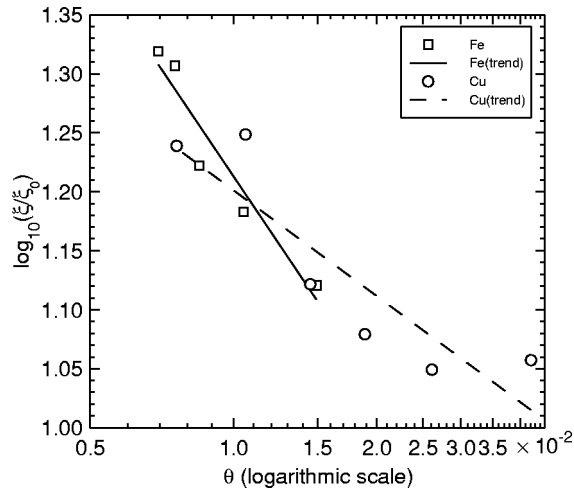


FIG. 2. Correlation length ξ vs normalized strain-hardening rate θ .

interaction value $|g_4| = 0.61 \pm 0.25$ is consistent with that determined from α , $|g_4| = 0.40 \pm 0.19$.

In copper, due to a significantly greater value of the fundamental scale ξ_0 , the scope of the fractal approximation is narrower. The dimensionality (changes from $D = 1.27 \pm 0.03$ to $D = 1.34 \pm 0.01$) and absolute interaction $|g_4| = 1.14 \pm 0.073$ differ from the corresponding values for iron. On the other hand, the obtained absolute interaction is not consistent with the estimate $|g_4|_{\text{est}} = 0.88 \pm 0.02$ deduced from α using Eq. (7). A possible reason for this difference is

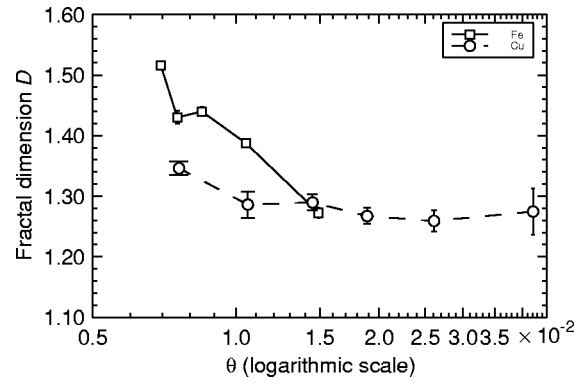


FIG. 3. Fractal dimension of the correlation function of displacement field fluctuations vs normalized strain-hardening rate θ .

that “nonclassical” behavior—fractality—arises in the second order of perturbation theory, the same order needed in renormalization (7) for index α .

IV. CONCLUSIONS

Surface topology investigations reveal the statistics of the displacement field during plastic deformation of real engineering materials. The numerical values and analytic behavior of some parameters, grounded in experimental data, are consistent with those obtained from proposed concepts of instability. We have calculated the fundamental length scale ξ_0 and the interaction magnitude g_4 —important model constants connecting the singular behavior of mesoscopic perturbations to features of the stress-strain diagram.

¹There are many works; see, e.g., F. A. Bandak, R. W. Armstrong, and A. S. Douglas, *Phys. Rev. B* **46**, 3228 (1992); N. I. Gershenson, *ibid.* **50**, 13 308 (1994).

²P. Hähner and M. Zaiser, *Acta Mater.* **45**, 1067 (1997).

³E. Cosserat and F. Cosserat, *Théorie des Corps Déformables* (Hermann, Paris, 1909); R. A. Toupin, *Arch. Ration. Mech. Anal.* **16**, 87 (1964).

⁴L. Limat, *Phys. Rev. B* **37**, 672 (1988).

⁵R. D. Mindlin, *Arch. Ration. Mech. Anal.* **16**, 51 (1964).

⁶A. E. Green and R. S. Rivlin, *Arch. Ration. Mech. Anal.* **17**, 113 (1964).

⁷A. D. Amit, *Field Theory, the Renormalization Group, and Critical Phenomena* (McGraw-Hill, New York, 1978).

⁸W. Prager, *J. Appl. Mech.* **15**, 226 (1948).

⁹A. M. Avdeenko, *Izv. Akad. Nauk. SSSR, Met.* **2**, 64 (1992).

¹⁰A. M. Avdeenko, M. A. Shtremel, and E. I. Kuzko, *Fiz. Tverd. Tela (Leningrad)* **37**, 3751 (1995); *Phys. Solid State* **37**, 2069 (1995).